Second moment modelling of conjugate turbulent heat transfer in porous media

doi: https://doi.org/10.1615/IHTC16.cov.022401

Proceedings of the 16th International Heat Transfer Conference, IHTC-16
August 10–15, 2018, Beijing, China

IHTC16-22401

SECOND MOMENT MODELLING OF CONJUGATE TURBULENT HEAT TRANSFER IN POROUS MEDIA

Y. Kuwata[1,*] & K. Suga[1]

[1]Department of Mechanical Engineering, Osaka Prefecture University, Gakuen-cho 1-1, Naka-ku, Sakai, Osaka 599-8531, Japan

ABSTRACT

To predict conjugate turbulent heat transfer inside porous media, double (volume and Reynolds) averaged energy equations of fluid and solid phases are modelled based on the multi-scale second moment closure. Unknown correlation such as the volume averaged turbulent heat flux, dispersion heat flux, wall-heat transfer and tortuosity terms arise in the double averaged energy equations. The wall-heat transfer term is modelled considering the analogy between the flow and thermal fields. For the heat fluxes, several heat flux models such as eddy viscosity model, generalized gradient diffusion hypothesis (GGDH) and higher order GGDH model are assessed. The developed model is evaluated by comparing the large eddy simulation results of fully developed conjugate heat transfer in square rod arrays, staggered cube arrays and body centred cubic matrix foam. It is confirmed that the higher order GGDH heat flux model shows the best performance in prediction of thermal fields, and the wall-heat transfer based on the analogy to the modelling strategy of the drag term successfully works. It is found that the present model can reasonably predict the macroscopic temperature profiles of solid and fluid phases.

KEY WORDS: porous media, double averaging, turbulence, second moment closure

1. INTRODUCTION

Since porous media have large contact area per volume leading to high heat and mass transfer performance, they are widely utilized for heat exchangers, catalytic reactors and fluidized beds [3, 7]. Accordingly, simulating heat and mass transfer inside porous media is crucial in many engineering designs.

In engineering computational fluid dynamics analyses of porous medium flows, the volume averaging theory [13, 14] is usually applied since precisely describing the shape of each pore or grain element of porous media requires despairingly huge computer costs. To analyze heat transfer in porous media, the non-equilibrium model which solves two energy equations for fluid and solid phases have been developed since the solid and fluid phase temperatures are not equilibrium in many occasions. Furthermore, when the flows become turbulent, the Reynolds averaging should be also applied to the volume averaged equations. However, this double (Reynolds and volume) averaging process produces many unknown correlations. To close the double averaged momentum equation, [6, 8] modelled the volume averaged Reynolds stress by k-ε eddy viscosity model by utilizing the simulation data for turbulence in rod bundles. However, their model neglected an influence of velocity dispersions, and many correlations in the transport equation for k were dropped without sufficient discussions. For more elaborate model, [5] developed a model based on the two-component-limit (TCL) second moment closure of [1]. They confirmed the validity of their developed model for fully-developed porous

*Corresponding Y. Kuwata: kuwata@me.osakafu-u.ac.jp

medium flows and interface turbulence between a porous/fluid region. Furthermore, it was reported that turbulence anisotropy, which was significantly important to predict turbulent heat and mass transfer, was correctly reproduced.

As well as the double averaged momentum equation, many unknown terms arises in double averaging energy equations, namely, turbulent and dispersion heat fluxes, wall-heat transfer and turtuosity terms. For the volume averaged turbulent heat flux, [9] modelled it by the eddy diffusivity concept, while they modelled the dispersion heat flux by the gradient diffusion model with a function of the Peclet number. [4] modelled the volume averaged turbulent heat flux by the generalized gradient diffusion hypotheses (GGDH) coupled with the multi-scale second moment closure of [5]. [8] discussed effects of the dispersion heat flux through the turbulent heat transfer simulations in rod bundles with the k-ε turbulence model. To obtain the correlation for the wall heat transfer which exchanges energy between the fluid and solid phases, [10] analyzed square rod array flows using the k-ε turbulence model. More recently, development of the computer technology has made it possible to perform large eddy simulation (LES) of turbulent porous medium flows. LESs of conjugate turbulent heat transfer inside square rod arrays, staggered cube arrays and body-centered-cube foam were carried out by [11] to evaluate modelling strategy of the turbulent and dispersion heat fluxes. Their priori test suggested that the higher-order extension of the GGDH model could improve prediction performance for dispersion and turbulence heat fluxes.

In this research, utilizing the latest LES data of [11], the dispersion and turbulent heat fluxes, and the wall-heat transfer terms are modelled coupled with the multi-scale second moment closure of [5]. The proposed model equations are validated in the conjugate thermal fields of flows through square rod arrays, staggered cube arrays and body centred cubic foam.

2. TURBULENCE MODELLING

2.1 Double-averaged transport equations

Following [13, 14], the volume averaging process in the porous media is applied to the Navier-Stokes and energy equations. The volume averaged value $\langle\phi\rangle$ is called the *superficial* averaged value while $\langle\phi\rangle^f$ is the *intrinsic* averaged value of a variable ϕ. Between them, the relation: $\langle\phi\rangle = \varphi\langle\phi\rangle^f$, exists with the porosity of the porous medium φ. When the Reynolds averaging is performed to the volume averaged momentum equation for incompressible flows in porous media, by defining the dispersion: $\tilde{\phi} = \phi - \langle\phi\rangle^f$, the Reynolds averaged value: $\overline{\phi}$ and the fluctuation: $\phi' = \phi - \overline{\phi}$, the resultant form can be written as

$$\begin{aligned}\frac{\partial\langle\overline{u}_i\rangle^f}{\partial t} + \langle\overline{u}_k\rangle^f\frac{\partial\langle\overline{u}_i\rangle^f}{\partial x_k} &= -\frac{1}{\rho}\frac{\partial\langle\overline{p}\rangle^f}{\partial x_i} + \frac{\partial}{\partial x_k}\left(\nu\frac{\partial\langle\overline{u}_i\rangle^f}{\partial x_k}\right) \\ &\quad -\overline{f}_i - \frac{\partial}{\varphi\partial x_k}\varphi(\underbrace{\langle\overline{\langle u_i'u_k'\rangle}^f}_{R_{ik}^A} + \underbrace{\langle\tilde{\overline{u}}_i\tilde{\overline{u}}_k\rangle^f}_{\mathcal{T}_{ik}}) + \underbrace{\frac{\nu}{\varphi}\left(\frac{\partial\varphi}{\partial x_k}\frac{\partial\langle\overline{u}_i\rangle^f}{\partial x_k} + \langle\overline{u}_i\rangle^f\frac{\partial^2\varphi}{\partial x_k^2}\right)}_{\overline{g_i^\varphi}},\end{aligned} \tag{1}$$

where u_i, p, ρ, and ν are the fluid velocity, pressure, density and kinematic viscosity, respectively. The drag term f_i consists of the viscous drag and the form drag. The term $\overline{g_i^\varphi}$ arises due to the inhomogeneity of the porosity. The unknown covariant terms: $\langle\tilde{\overline{u}}_i\tilde{\overline{u}}_k\rangle^f$ and $\langle\overline{u_i'u_k'}\rangle^f$, are respectively the dispersive covariance (dispersion stress) $\mathcal{T}_{ik}$ and the volume averaged Reynolds stress R_{ik}^A. The volume averaged Reynolds stress can be decomposed into the macro-scale Reynolds stress R_{ij} and the micro-scale Reynolds stress r_{ij}:

$$R_{ij}^A = \underbrace{\overline{\langle u_i'\rangle^f\langle u_j'\rangle^f}}_{R_{ij}} + \underbrace{\overline{\langle\tilde{u}_i'\tilde{u}_j'\rangle^f}}_{r_{ij}}. \tag{2}$$

Since the volume averaged Reynolds stress is the sum of the macro-scale and micro-scale Reynolds stresses, it is called the total Reynolds stress hereafter. The presently used multi-scale second moment closure, which is based on the two-component limit (TCL) second moment closured developed by [1], solves the transport equation of R_{ij}^A while its micro-scale part r_{ij} and the dispersive covariance $\mathcal{T}_{ik}$ are respectively modelled by the two-equation eddy viscosity model and the algebraic expressions. See [5] for detailed model formulations and validation in fully-developed porous medium flows.

Energy of the solid and fluid phases is not always in equilibrium. Hence, the two-energy equation model solving the energy equations of two phases individually needs to be considered. By applying the volume and Reynolds averaging to the energy equations for fluid and solid phases, the double averaged energy equations can be derived as

for fluid phases:

$$\frac{\partial \varphi \langle \overline{T_f} \rangle^f}{\partial t} + \varphi \langle \overline{u}_j \rangle^f \frac{\partial \langle \overline{T_f} \rangle^f}{\partial x_j} = \frac{\partial}{\partial x_j}\left(k_f \frac{\partial \varphi \langle \overline{T_f} \rangle^f}{\partial x_j} \right) - \frac{\partial}{\partial x_j}\left\{ \varphi \left(\underbrace{\overline{\langle u_j' T_f' \rangle^f}}_{H_j^A} + \underbrace{\langle \tilde{\overline{u}}_j \tilde{\overline{T_f}} \rangle^f}_{\mathcal{H}_j} \right) \right\} + \underbrace{\frac{\partial}{\partial x_j}\left(\frac{1}{\Delta V} \int_A n_j k_f \overline{T_f} dA \right)}_{S_{Tf}} + \underbrace{\frac{1}{\Delta V} \int_A n_j k_f \frac{\partial \overline{T_f}}{\partial x_j} dA}_{S_{Wf}}, \quad (3)$$

for solid phases:

$$\frac{\partial (1-\varphi) \langle \overline{T_s} \rangle^s}{\partial t} = \frac{\partial}{\partial x_j}\left(k_s \frac{\partial (1-\varphi) \langle \overline{T_s} \rangle^s}{\partial x_j} \right) - \underbrace{\frac{\partial}{\partial x_j}\left(\frac{1}{\Delta V} \int_A n_j k_s \overline{T_s} dA \right)}_{S_{Ts}} - \underbrace{\frac{1}{\Delta V} \int_A n_j k_s \frac{\partial \overline{T_s}}{\partial x_j} dA}_{S_{Ws}}, \quad (4)$$

where $\langle T_f \rangle^f$ and $\langle T_s \rangle^s$ denote the intrinsic averaged energy of fluid and solid phases, respectively. The sub- and superscripts of "f" and "s" denote the fluid and solid phases, respectively. Note that ΔV, A and n_j are the local averaging volume, superficial area of the solid phase and its unit normal vector pointing outward from the fluid to the solid phase, respectively. The fluid and solid thermal diffusivities are k_f and k_s. The volume averaged turbulent heat flux $H_j = \overline{\langle u_j' T_f' \rangle^f}$ and the dispersion heat flux (thermal dispersion) $\mathcal{H}_j = \langle \tilde{\overline{u}}_j \tilde{\overline{T_f}} \rangle^f$, which are unknown terms, arise in Eq.(3). The surface integration terms are the tortuosity S_T and the wall heat transfer (interfacial heat transfer) S_W which take account of the energy exchange between the fluid and solid phases in Eqs.(3) and (4). Since the contribution of the tortuosity is less significant compared with the other unknown terms such as the volume averaged turbulent heat flux, the dispersion heat flux and the wall-heat transfer terms, the present study attempts to model H_j^A, $\mathcal{H}_j$ and S_W.

2.2 Modelling turbulence and dispersion heat fluxes

The volume averaged turbulence heat flux and the dispersion heat flux are usually modelled by the eddy viscosity model (EVM) [9]. However, it is well known that the EVM fails to take account of the turbulence/dispersion anisotropy despite the fact that turbulence/dispersion anisotropy plays significantly important role in energy transfer. To reflect the influence of turbulence/dispersion anisotropy, the GGDH (generalized gradient diffusion hypothesis) flux model of [2], which includes the stress tensor, is preferably employed in conjunction with the Reynolds stress resolving model. Following [11], sum of the volume averaged turbulent heat flux and the dispersion heat flux can be modelled as the GGDH model:

$$H_i + \mathcal{H}_i = -c_\theta \frac{\langle k \rangle^f}{\langle \varepsilon \rangle^f} R_{ij} \frac{\partial \langle \overline{T_f} \rangle^f}{\partial x_j} - c_\theta' \frac{\mathcal{K}}{\mathcal{E}} \mathcal{T}_{ij} \frac{\partial \langle \overline{T_f} \rangle^f}{\partial x_j}, \quad (5)$$

where the model constants of $c_\theta = 0.5$ and $c'_\theta = 0.08$ are used, and k, ε, $\mathcal{K}$ and $\mathcal{E}$ are the volume averaged turbulence energy: $k = R_{kk}/2$, its dissipation rate, the dispersion energy: $\mathcal{K} = \mathcal{T}_{kk}/2$ and its dissipation rate, respectively. Although it was confirmed by the a priori test of [11] with their LES data that prediction performance of the GGDH model was better than the that of the EVM, there was still difficultly to predict in several types of porous media with wide range of porosity and further extended version of the higher-order GGDH model (HOGGDH):

$$H_i + \mathcal{H}_i = -c_\theta \frac{\langle k \rangle^f}{\langle \varepsilon \rangle^f} \frac{R_{ik}R_{kj}}{k} \frac{\partial \langle \overline{T_f} \rangle^f}{\partial x_j} - c'_\theta \frac{\mathcal{K}}{\mathcal{E}} \frac{\mathcal{T}_{ik}\mathcal{T}_{kj}}{\mathcal{K}} \frac{\partial \langle \overline{T_f} \rangle^f}{\partial x_j}, \tag{6}$$

could improve the prediction. Accordingly, the present study employs the HOGGDH model with the multi-scale second moment closure.

2.3 Modelling wall-heat transfer term

Since the wall-heat transfer term exchanges energy between solid and fluid phases, precise modelling of this effect is crucial to predict non-equilibrium thermal fields. Traditionally, the wall-heat transfer term is modelled

$$S_{Wf} = \frac{\alpha A}{\Delta V} \left(\langle \overline{T_f} \rangle^f - \langle \overline{T_s} \rangle^s \right), \tag{7}$$

where α is the wall heat transfer coefficient. The wall heat transfer coefficient has been estimated for the certain field by referring to the corresponding data. Using experimental correlation for packed beds, [12] modelled the wall heat transfer coefficient by the Reynolds number based on the Darcian velocity and the particle diameter. For more analytical strategy, [4] developed a wall heat transfer model by analogy to the modelling strategy of the viscous drag term. Their model included the permeability instead of the particle diameter. Through validation in laminar/turbulence heat transfer in square rod array flows, they demonstrated very good performance in wide range of porosity and Reynolds number. The present study attempts to extend the model of [4] assuming the similarity between the flow and thermal fields, and evaluate in the other types of porous media. The wall heat transfer term is written as

$$S_{Wf} = \frac{k_f A}{L \Delta V} Nu \left(\langle \overline{T_f} \rangle^f - \langle \overline{T_s} \rangle^s \right), \tag{8}$$

where Nu is the Nusselt number, L is the representative length scale for porous media. Assuming the similarity between the flow and thermal fields, Nusselt number can be related to a friction coefficient C_f:

$$Nu \sim \frac{1}{2} C_f Re Pr^{1/3}, \tag{9}$$

where the Reynolds number Re is defined as $Re = \langle U \rangle L/\nu$, Pr denotes the Prandtl number. The friction coefficient for the porous media is expressed by a pressure drop ΔP as

$$C_f = \frac{\langle \Delta P \rangle}{0.5 \rho \langle U \rangle^2} \sim \frac{L}{0.5 \langle U \rangle^2} \frac{\varphi}{\rho} \frac{\Delta \langle P \rangle^f}{L}. \tag{10}$$

In fully developed porous medium flows, the volume averaged pressure gradient is balanced with the drag force term f. Thus, Eq. (10) becomes

$$C_f \sim \frac{L}{0.5 \langle U \rangle^2} f, \tag{11}$$

Substituting Eqs.(9) and (11) for Eq.(8), the wall heat transfer term can be expressed as

$$S_{Wf} \sim \frac{k_f A \varphi}{\langle U \rangle^2 \Delta V} f Re Pr^{1/3} \left(\langle \overline{T_f} \rangle^f - \langle \overline{T_s} \rangle^s \right). \tag{12}$$

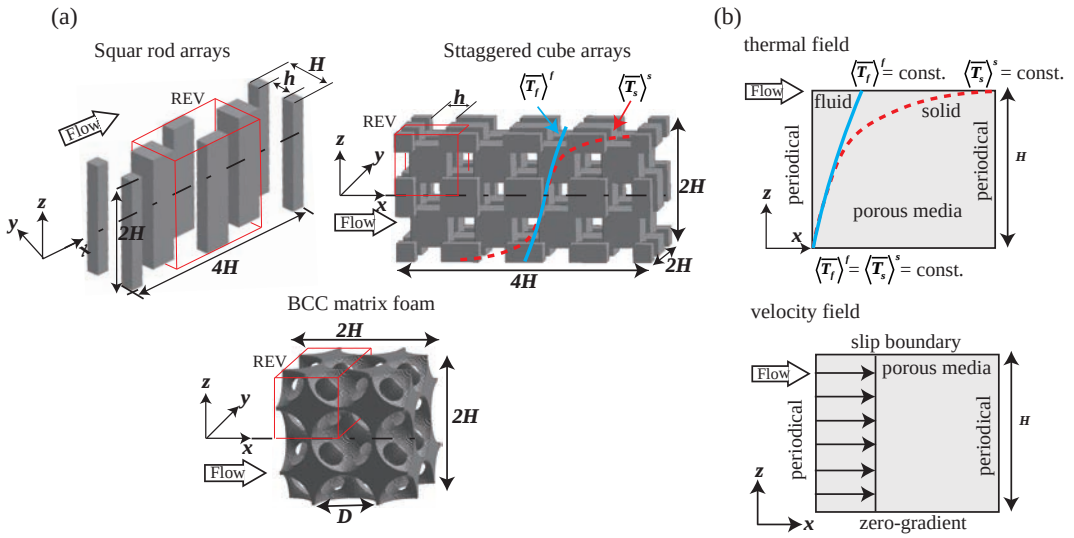

Fig. 1 Computational geometry: (a) microscopic LES by [11], (b)statistical thermal fields for macroscopic computations.

When the Dracy-Forchheimer model is used for the drag force term, the wall heat transfer term can be rewritten as

$$S_{Wf} \sim \frac{k_f A L \varphi}{\Delta V}\left(\frac{1}{K}+\frac{C^F\langle U\rangle}{\nu\sqrt{K}}\right) Pr^{1/3}\left(\langle\overline{T_f}\rangle^f-\langle\overline{T_s}\rangle^s\right). \tag{13}$$

When the representative length L is assumed to be pore diameter, the product of the surface ares A and L represents the volume of pores in the representative elementary volume (REV). Hence, the volume ratio may be expressed as $AL/\Delta V \sim \varphi$. Assuming that the representative length L can be the same order of $\sqrt{K}$, the wall-heat transfer term can be expressed as

$$S_{Wf} \sim \frac{k_f \varphi^2}{K}\left(1+C^F\frac{\sqrt{K}\langle U\rangle}{\nu}\right) Pr^{1/3}\left(\langle\overline{T_f}\rangle^f-\langle\overline{T_s}\rangle^s\right). \tag{14}$$

Using the tensorial expression for the permeability and the Forchheimer coefficient, the resultant form of the wall-heat transfer model is expressed as

$$S_{Wf} = C_{w1} k_f \varphi^2 K^{ij} L_{ij}\left(1+C_{w2}L_{ij}C_{ij}^F \hat{Re}_K\right) Pr^{1/3}\left(\langle\overline{T_f}\rangle^f-\langle\overline{T_s}\rangle^s\right). \tag{15}$$

where K^{ij} is the inverse matrix of the permeability tensor K_{ij}, C_{ij}^F is the Forchheimer tensor, and L_{ij} is defined as $L_{ij} = \ell_i\ell_j$, $\ell_i = \langle\overline{u_i}\rangle^f/\sqrt{\langle\overline{u_k}\rangle^f\langle\overline{u_k}\rangle^f}$ The permeability Reynolds number $\hat{Re}_K$ is defined as $\hat{Re}_k = \sqrt{K^*_{kk}}\sqrt{\langle\overline{u_k}\rangle^f\langle\overline{u_k}\rangle^f}/\nu$. Here, $K^*_{ij} = (K_{ik}L_{kj}+K_{jk}L_{ki})/2$. The model constants presently used are $C_{w1} = 0.23$ and $C_{w2} = 0.07$.

3. APPLICATION RESULTS AND DISCUSSIONS

The calibration of the present model is performed in fully developed turbulent flows inside square rod arrays (SRA), staggered cube arrays (SCA) and BCC foam whose schematic diagrams and their REV are illustrated in Fig.1. For the validation, conjugate heat transfer LES data of [11] are used as reference data. The representative length for the Reynolds number is a gap between square rods/cubes : h in cases SRA and SCA while the pore

Table 1 Flow condition and characteristics parameters of porous media.

Case	Re	φ	K_{xx}/H^2	$C_{F,xx}$
SRA	3000	0.897	3.23×10^{-2}	0.114
		0.823	1.71×10^{-2}	0.161
SCA	3000	0.711	5.13×10^{-3}	0.102
		0.576	2.33×10^{-3}	0.139
BCC	700	0.909	8.50×10^{-3}	0.225
		0799	2.72×10^{-3}	0.686

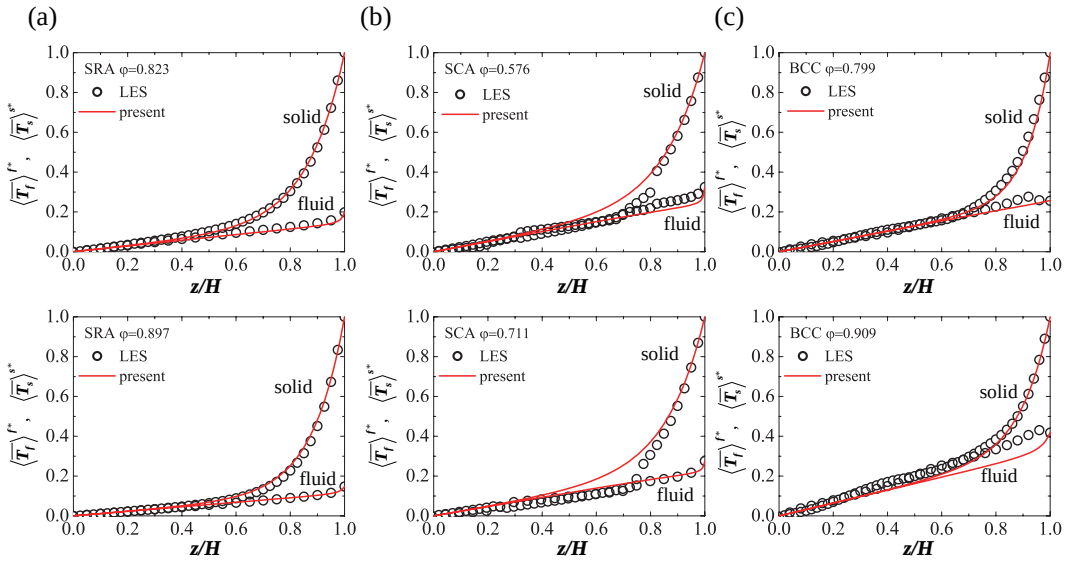

Fig. 2 Comparison of the mean temperature profiles of the solid and fluid phase; (a) square rod array, (b) staggered cube array, (c) BCC foam. The normalized temperatures $\langle T_f \rangle^{f*} = (\langle \overline{T_f} \rangle^f - \langle \overline{T_f} \rangle^f_{z/H=0})/(\langle \overline{T_s} \rangle^s_{z/H=1} - \langle \overline{T_f} \rangle^f_{z/H=1})$ and $\langle T_s \rangle^{s*} = (\langle \overline{T_s} \rangle^s - \langle \overline{T_s} \rangle^s_{z/H=0})/(\langle \overline{T_s} \rangle^s_{z/H=1} - \langle \overline{T_f} \rangle^f_{z/H=1})$.

diameter is used for BCC foam. In microscopic LES in [11], the periodical boundary conditions were applied to the streamwise (x) and cross-streamwise (y) directions while constant temperatures are imposed for the solid phase (T_{Hot}, T_{Cool}) at the top ($z/H = 1$) and the bottom ($z/H = -1$) boundaries, and the adiabatic free slip condition were imposed to the top and bottom fluid phase boundaries. The macroscopic simulation assumes the homogeneous media. The number of computational grid nodes for the macroscopic computations are $15(x) \times 50(z)$ for the two-dimensional computational domain of $H(x) \times H(z)$. Periodical boundary conditions are imposed at the streamwise direction. For the cross-streamwise boundary faces ($z/H = 1$), LES data of the solid and fluid phase temperatures are imposed whereas the slip boundary condition is considered for the flow fields as shown in Fig.1(b). Since the solid and fluid temperatures reach an equilibrium state at $z/H = 0$, the bottom boundary temperature of the fluid phase is set to be the same as the solid phase temperature and the zero-gradient conditions are applied to the velocity field. Following the LES study, the ratio of the thermal diffusivities $k_s/k_f = 4.4$, which corresponds to the ratio of aluminium/air, is applied. The flow conditions and characteristic parameters of the porous media needed for the macroscopic computations are listed in Table 1. (In the present cases, the permeability and Forchheimer tensors are diagonal.)

Figure 2 shows comparisons of the mean temperature profiles between the predicted results and the LES data. As approaching the symmetry plane at $z/H = 0$, thermal field goes to the equilibrium state due to the role of the energy exchanging terms: S_{w_f} and S_{w_s}. This trend is successfully captured by the present model,

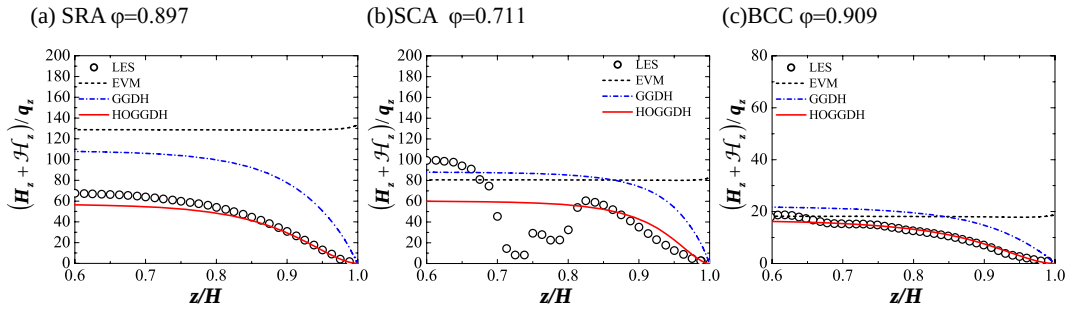

Fig. 3 Comparison of the volume averaged turbulent hean flux and the dispersion heat flux; (a) square rod array of $\varphi = 0.897$, (b) staggered cube array of $\varphi = 0.711$, (c)bcc foam of $\varphi = 0.909$.

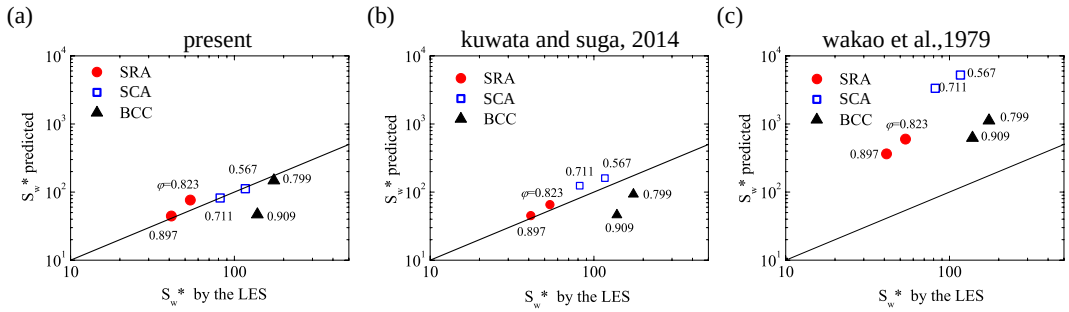

Fig. 4 Comparison of the wall-heat transfer term; (a) present model, (b) model by [4] (c) model by [12]. The normalized wall-heat transfer is $S_w^* = S_w H^2 / \left(\langle T \rangle^s - \langle T \rangle^f \right) / k_f$.

which demonstrate that the developed wall-heat transfer model can reasonably reproduce the energy exchange between the solid and fluid phases. It should be noted that the LES data are intrinsically averaged over $x-y$ plane and thus show discontinuous/wavy profiles in z direction corresponding to the porous structures, which is clearly seen in porous media with three-dimensional structures in cases SCA and BCC. However, since the present macroscopic model solves volume averaged values in the REV, the present model cannot predict the discontinuous/wavy distribution within the REV. Thus slight discrepancies between the LES data and predicted results can be appeared. However, it is confirmed that overall agreement with the LES data is satisfactory in all types of the porous media.

In order to evaluate the model in detail, Fig.3 compares sum of the dispersion heat flux $\mathcal{H}_z$ and the volume averaged turbulent heat flux H_z normalized by the heat flux: $q_x = -k_f \partial T / \partial y$. Since the wall-normal mean and fluctuated velocity reduce to zero at the slip wall of $z/H = 1$, both $\mathcal{H}_z$ and H_z become zero at the slip boundary. Since the GGDH and HOGGDH models include the volume averaged Reynolds stress/dispersive covariance tensor, the behaviour near the slip wall is successfully captured. On the other hand, the eddy viscosity/diffusivity model does not include the stress tensors, and it thus fails to reproduce that behaviour near the slip wall. It is confirmed that prediction results of the limiting behaviour near the slip walls by the HOGGDH are obviously better than those by the GGDH model. The LES data in case SCA is significantly damped near $0.65 < z/H < 0.85$ resulting from the blocking effects of the velocity fluctuation in z direction due to the presence of the cube faces normal to z direction. However, again, since the present macroscopic model solves volume averaged values in the REV, such behaviour cannot be predicted.

Comparisons of the volume averaged wall-heat transfer terms between the present model, the other models of [4, 12] and the LES data are presented in Fig.4. Note that although the model of [12] requires the mean particle diameter, it is difficult to be determined for BCC foams. Alternatively, the root mean square of the permeability $\sqrt{K_{xx}}$ surrogates the particle diameter. It is found that the wall-heat transfer model of [12] significantly over

predicts the wall-heat transfer. Although prediction by the model by [4] is considerably better than that by the model of [12], the results in case SCA are still overpredicted and the results in case BCC are underpredicted as shown in Fig.4(a) and (b). It is confirmed that the presently developed model successfully improves the prediction accuracy compared with the model of [4]. However, the presently developed model still underpredicts in case BCC at $\varphi = 0.909$. The reason is that since the thermal field in case BCC at $\varphi = 0.909$ by the LES reaches almost the equilibrium state at $z/H = 0.7$ as shown in Fig.2(c) mean that the energy exchange dominantly works in the limited in the REV ($0.7 < z/H < 1$), S_w by the LES data may not represent the volume averaged values in the REV.

4. CONCLUSIONS

To macroscopically simulate turbulent heat transfer inside porous media, unknown correlations appearing in double (volume and Reynolds) averaged energy equations of fluid and solid phases are modelled coupled with the multi-scale second moment closure. The wall heat transfer term is modelled considering analogy between the flow and thermal fields while the dispersion and volume averaged turbulence heat fluxes are modelled by the higher order GGDH model. The developed model is evaluated by comparing the large eddy simulation results of fully developed conjugate heat transfer in square rod arrays, staggered cube arrays and body centred cubic foam. The prediction performance of the higher order GGDH heat flux model is confirmed to be better than that by the GGDH model, and the wall-heat transfer based on the analogy to the modelling strategy of the drag term successfully works in several types of the porous media. Thus, the present model can reasonably predict the macroscopic temperature profiles of solid and fluid phases.

REFERENCES

[1] Craft, T. J. and Launder, B. E., "A Reynolds stress closure designed for complex geometries," *Int. J. Heat Fluid Flow*, 17, pp. 246–254, (1996).

[2] Daly, B. J. and Harlow, F. H., "Transport equation in turbulence," *Phys. Fluids*, 13, pp. 2634–2649, (1970).

[3] de Lemos, M. J. S., *Turbulence in porous media*, Elsevier, UK, (2006).

[4] Kuwata, Y. and Suga, K., "Porous medium modeling of turbulent heat transfer in square rod arrays with multi-scale second moment closure," *Spec. Top. Rev. Porous Media: An International Journal*, 6, pp. 173–184, (2015).

[5] Kuwata, Y. and Suga, K., "Progress in the extension of a second-moment closure for turbulent environmental flows," *Int. J. Heat Fluid Flow*, 51, pp. 268–284, (2015).

[6] Nakayama, A. and Kuwahara, F., "A general macroscopic turbulence model for flows in packed beds, channels, pipes, and rod bundles," *J. Fluids Engrg.*, 130, pp. 101205–1–7, (2008).

[7] Nield, D. A. and Bejan, A., *Convection in porous media*, 3rd Edition, Springer, Berlin, (2006).

[8] Pedras, M. H. J. and de Lemos, M. J. S., "Macroscopic turbulence modeling for incompressible flow through undeformable porous media," *Int. J. Heat Mass Transfer*, 44, pp. 1081–1093, (2001).

[9] Pedras, M. H. J. and de Lemos, M. J. S., "Thermal dispersion in porous media as a function of the solid-fluid conductivity ratio," *Int. J. Heat Mass Transfer*, 51(21-22), pp. 5359–5367, (2008).

[10] Saito, M. B. and de Lemos, M. J., "A correlation for interfacial heat transfer coefficient for turbulent flow over an array of square rods," *J. Heat Transfer*, 128(5), pp. 444–452, (2006).

[11] Suga, K., Chikasue, R., and Kuwata, Y., "Modelling turbulent and dispersion heat fluxes in turbulent porous medium flows using the resolved les data," *Int. J. Heat Fluid Flow*, (2017).

[12] Wakao, N., Kaguei, S., and Funazkri, T., "Effect of fluid dispersion coefficients on particle-to-fluid heat transfer coefficients in packed beds. correlation of nusselt numbers," *Chem. Eng. Sci.*, 34(3), pp. 325–336, (1979).

[13] Whitaker, S., "Flow in porous media I: A theoretical derivation of Darcy's law," *Transp. Porous Med.*, 1, pp. 3–25, (1986).

[14] Whitaker, S., "The Forchheimer equation: A theoretical development," *Transp. Porous Med.*, 25, pp. 27–61, (1996).